

Experimental Study on Alternating Current Corrosion of Pipeline Steel in Alkaline Environment

Yan Yang, Shuli Wang, Chuang Wen*

School of Petroleum Engineering, Changzhou University, Zhonglou District, Changzhou, Jiangsu, 213016, China

*E-mail: chuang.wen@cczu.edu.cn

Received: 18 May 2016 / *Accepted:* 16 June 2016 / *Published:* 7 July 2016

The variation of the topsoil pH value in the X70 steel surface was studied under the AC corrosion process. The cyclic voltammetry technique was employed to investigate the AC action mechanism on the X70 pipeline steel in a soil environment. The results show that the alternating current has a great effect on the surface soil pH value. The corrosion mechanism of a metal suffered AC interference in an alkaline environment is that the AC changes the polarization potential and reduces the pH value of the surface soil. The coupling potential of the mixed alternating and direct currents presents a periodic oscillation in the electrode surface, which destroys the passivation of the X70 steel. The electrode surface is covered with a large amount of Fe (OH) ads, when the potential is in the range of the active dissolution potential of the X70 steel. In this condition, the hydroxides and oxides will form preferentially. In a different charge transfer process, the hydroxide, as the inhibitor of the passivation film, has an important impact on the metal corrosion. The increase of the corrosion rates is under the control of the transfer process.

Keywords: AC corrosion; alkaline environment; X70 steel; corrosion mechanism

1. INTRODUCTION

The study of corrosion on the mild steel or carbon steel is a very hot topic in the recent years [1-5]. The buried pipelines provided with high resistance coatings are susceptible to induction of AC voltage from paralleling high-voltage AC power lines. This AC voltage can cause a corrosion problem at coating defects where the AC current escapes the pipe, even if the pipeline has adopted the cathodic protection (CP) measures. The electrochemical behavior of AC interference on a steel or other metal aroused the interests of some investigators and engineers. Many studies have been focused on the acidic [6, 7] and neutral [8, 9] environment. But the soil environment gradually basifies at CP pipe/soil

interface, due to the decrease of the reaction of the cathodic hydrogen ions. When the cathodic protection current and AC interference current exist simultaneously, the pH at the steel / soil interface may change, and AC causes temperature rise at the steel/soil surface. High temperature and strong alkali environment have a major impact on the electrochemical corrosion behavior of metals. The mechanism of AC corrosion is different from the direct current (DC) corrosion [10-12]. Many theories have been developed to explain the mechanism of the action of AC corrosion, but it doesn't have a complete theory to explain this phenomenon of AC corrosion.

To clear the mechanism of AC corrosion, the variation of the pipeline/soil pH must be considered. It is well known that the electrochemical process of cathodic protection causes the environment around the cathode to become alkaline, especially at the surface of the metal protected. The pH value of typical pipeline surfaces with adequate CP would be in a range of 10 to 14 [13-15]. In the laboratory study [16], it was verified that the alkalization level of a cathodic metal/electrolyte interface submitted to AC currents depended on the protection potential value, the intensity of AC current, the level of confinement of the metal/electrolyte system and the electrolyte composition.

It is believed that the mechanism of AC induced corrosion involves the alkalisation of the local environment around a coating defect due to the enhancement of the cathode kinetics, etc., which creates the corrosive conditions in combination with an induced AC. If AC current is applied to a pipeline/soil system, the interface will be subjected alternatively to anodic and cathodic polarization. In the anodic cycle, corrosion will occur ($\text{Fe} \rightarrow \text{Fe}^{2+} + 2\text{e}^-$) and, in the cathodic cycle, the deposition of Fe^{2+} ions formed during the anodic cycle will occur, besides the reduction of H^+ ions and of dissolved O_2 .

The purpose of this project is to clarify the mechanisms of AC influenced corrosion of X70 pipeline steel. The electrochemical behaviour of X70 steel was investigated in deaerated simulated soil solution at pH 10~14 using traditional cyclic voltammetry (CV) in order to verify that the activation of iron occurs alternatively via a solid state reaction mechanism or via a dissolution/precipitation mechanism in different AC potentials.

2. EXPERIMENTAL PROCEDURE

2.1 Electrode and solution

The working electrode was X70 steel with the following chemical composition (in weight percent): 0.061% C, 1.53% Mn, 0.011% P, 0.0009% S, 0.24% Si and Fe balance. An X70 steel specimen size of 10 mm×10 mm×2.5 mm was embedded in Araldite, leaving one exposed surface of area 100 mm², as shown in Figure 1. The electrical contact was achieved through a thick copper wire soldered to the end of the specimen, but not exposed to the solution. The specimens were mechanically polished and then successively with finer SiC papers (800, 1000, 1200, 1600 grit) and Al₂O₃ (1 μm). Before the tests, the individual specimens were cleaned with acetone and de-ionized water.

A soil simulation solution (0.05 M/L NaHCO₃+0.1 M/L NaCl + 0.1 M/L Na₂SO₄) was prepared from distilled water and analytical grade (Merck) reagent for the electrochemical tests. The

deaeration of the soil simulation solution was achieved by bubbling highly pure nitrogen for 10 min before tests and still keep the ventilation state in the whole experiment process, to remove the oxygen in the solution.

The pH observation experiment used soil from the Qingdao bay area with the moisture content of 30%. Remove soil sieve rock solid impurities, such as loading container sealed with plastic wrap and set aside.

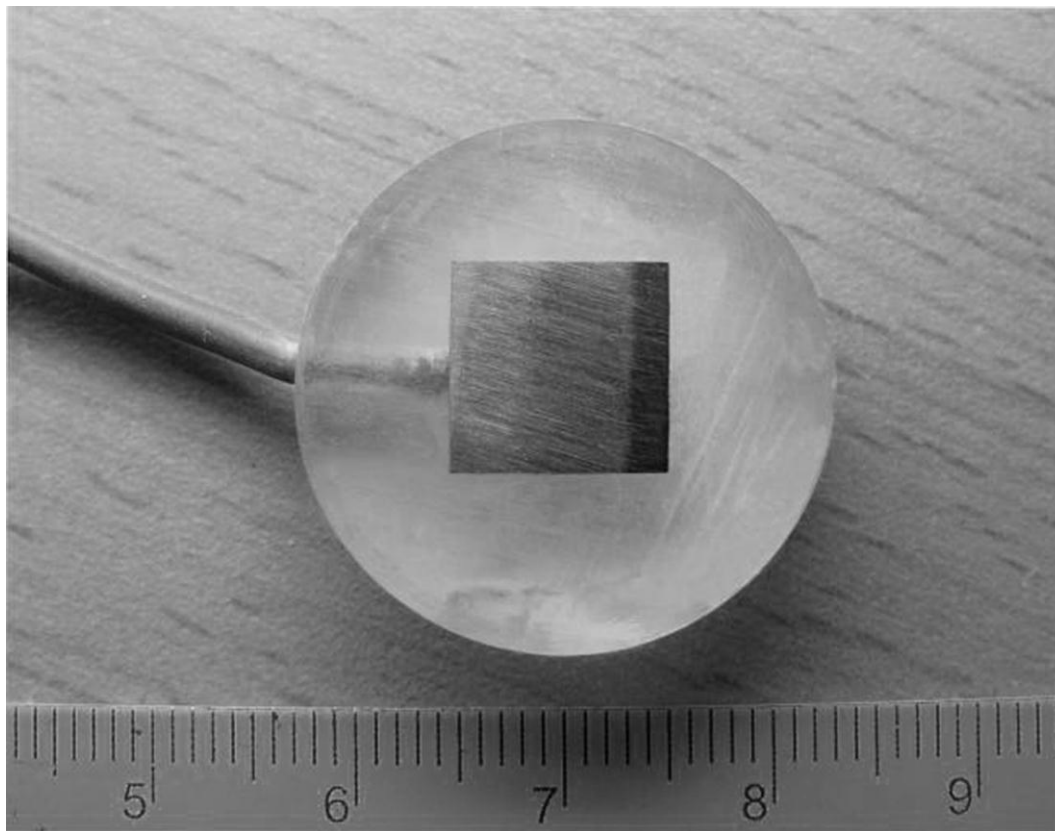


Figure 1. X70 steel specimens for AC corrosion

2.2 The pH measurements

A self-design device used for pH experiments is shown in Figure 2. A carbon electrode (1.5 cm in diameter) was used as an auxiliary electrode in the DC circuit, connecting an inductor (10 H) to isolate the AC interference. AC was provided by JJ98DD053A type variable frequency power supply. A titanium mesh electrode of 30 cm² was used as an auxiliary electrode in the AC circuit, connecting a capacitor (500 μ F) to isolate the DC interference. A portable soil pH meter IQ 150 produced in SPECTRUM was employed to measure the changes of pH value in the soil nearby the working electrode. The specimens were flat and pH meter surface were apart from of the specimens of 2 to 3 mm. To avoid uncertain influence factors such as temperature, the tests were implemented in a GDJS - 408 type constant temperature and humidity chamber. The temperature was set at 25 °C, and the humidity was controlled at 80%.

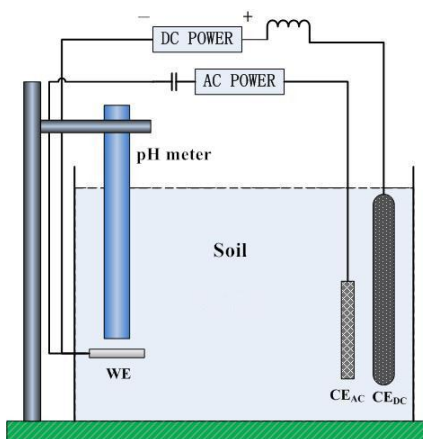
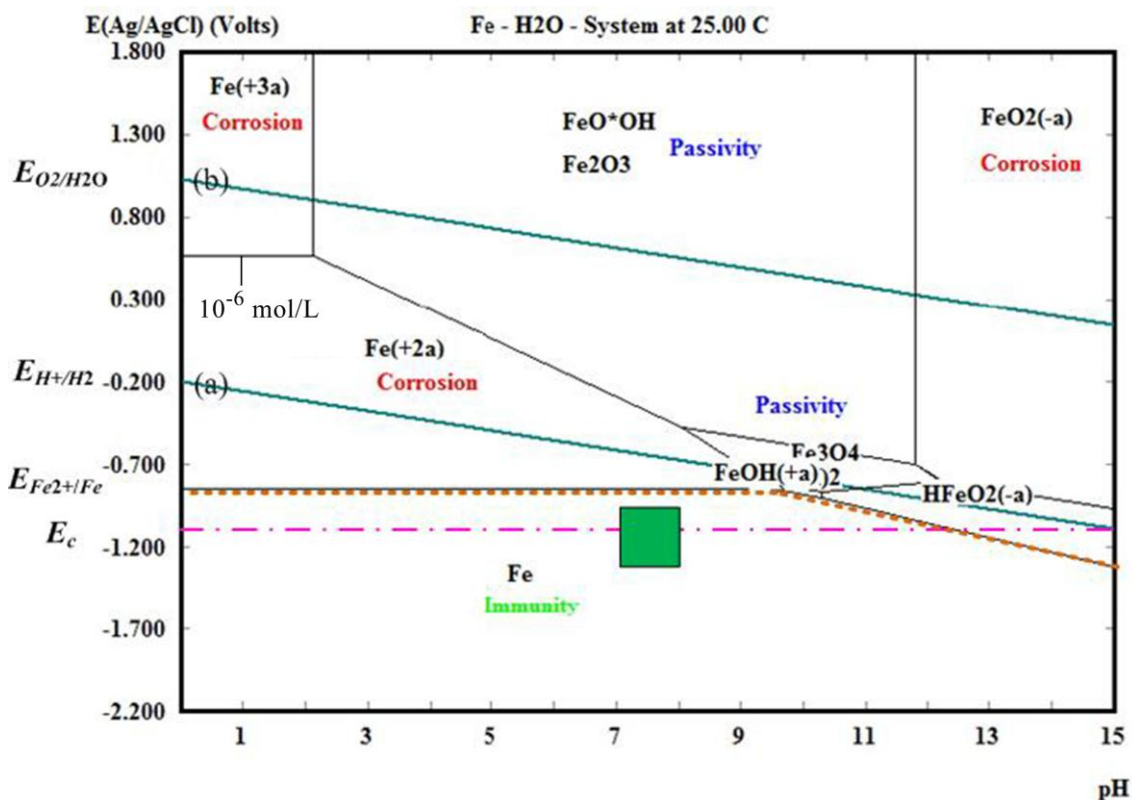
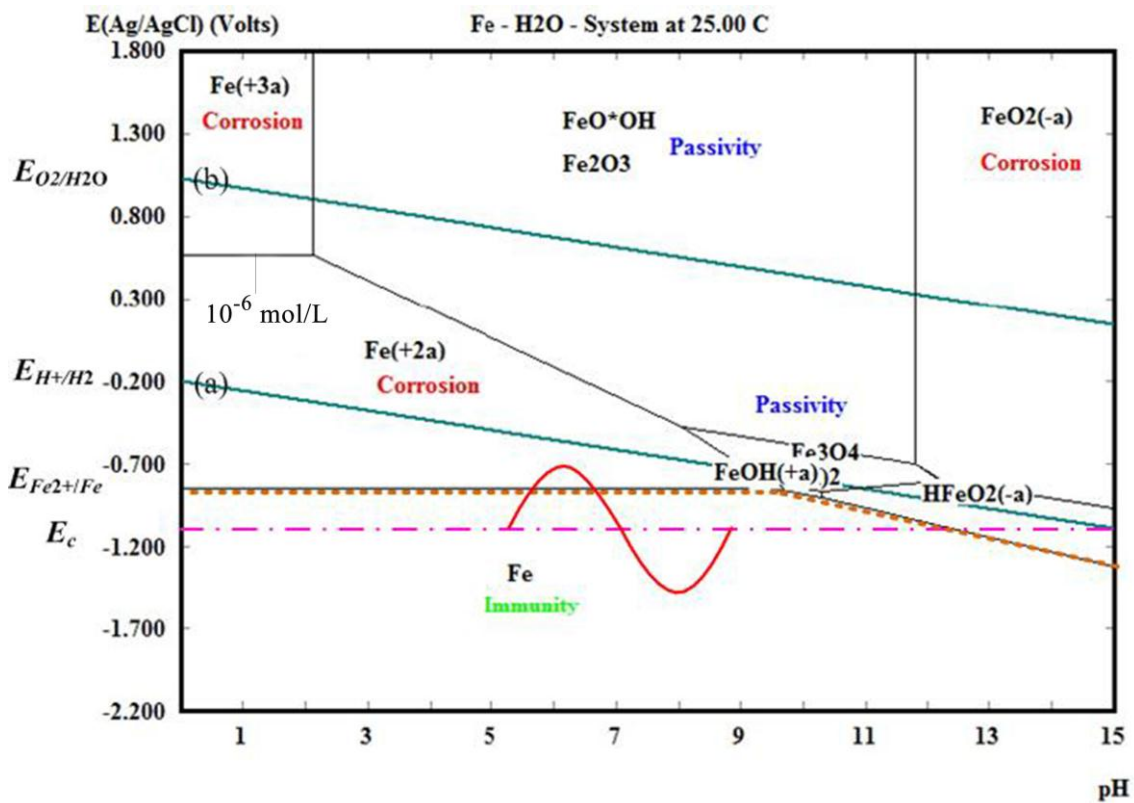


Figure 2. Schematic diagram of experimental setup for pH measurements of AC corrosion of X70 pipeline steel

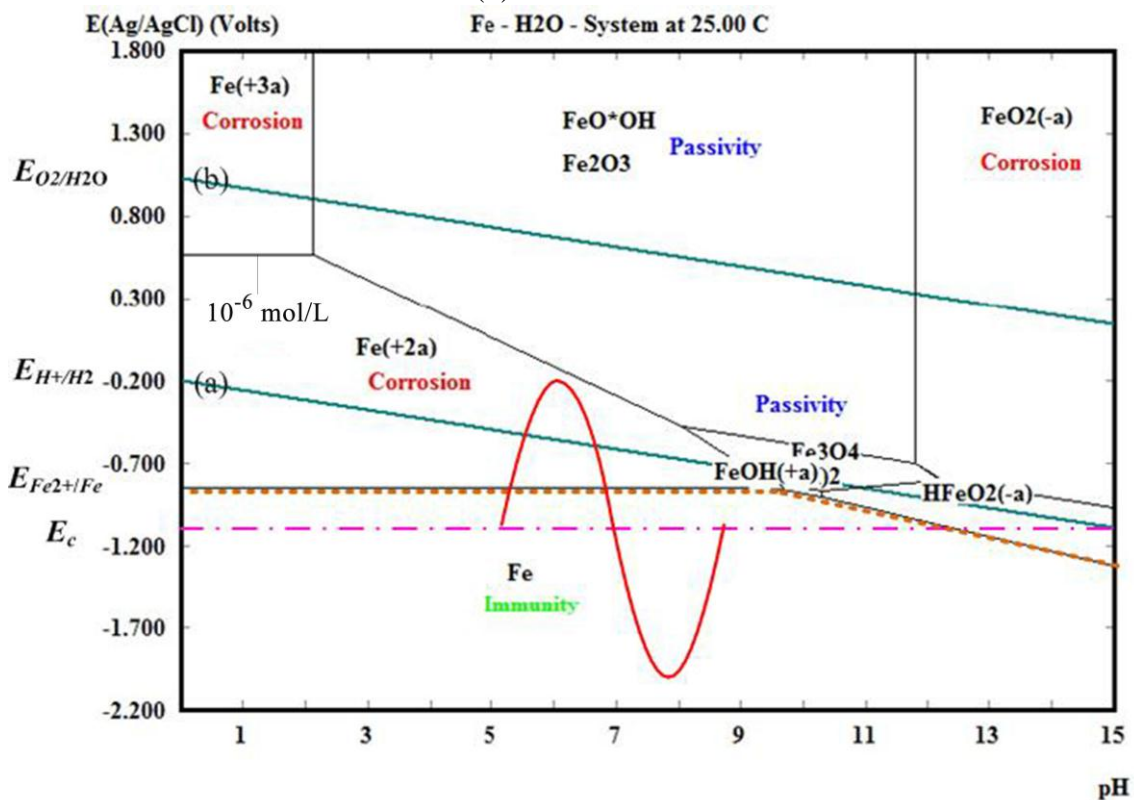
When a metal corrosion may occur, the corrosion thermodynamics conditions must be met. Based on this principle, Pourbaix mapped out the potential-pH curve according to the reaction of metal, oxygen, hydrogen and reaction thermodynamics data, also known as Pourbaix diagram. The diagram clearly differentiates from immunity, corrosion, passivity and other areas. The Cathodic Protection system was applied in the pipeline system based on this principle. In CP system, the metal will not be corroded, if the equilibrium potential of metal is in the immunity domain.



(a) Condition A



(b) Condition B



(c) Condition C

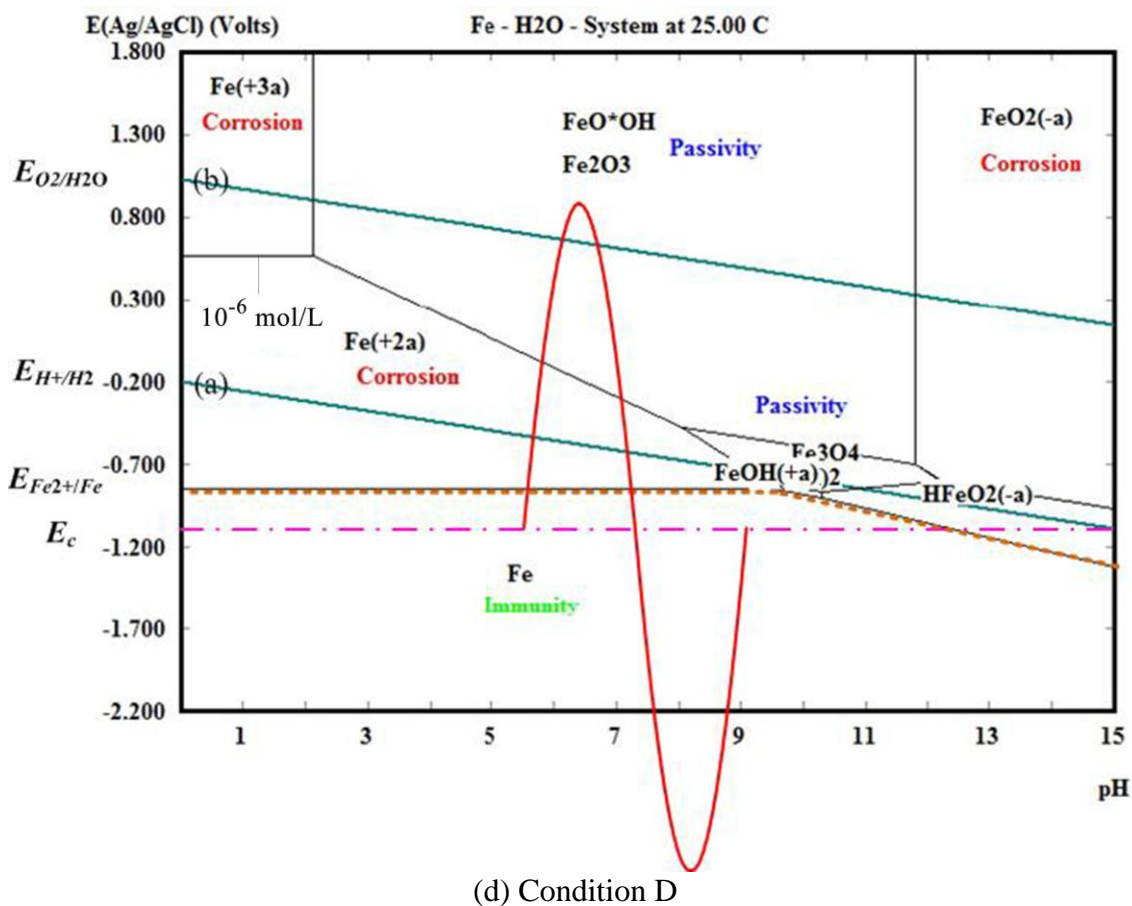


Figure 3. Pourbaix diagrams of four conditions adopted in CV tests

AC interference can be understood as the superposition of a positive and negative potential on the cathodic protection potential, making the metal corrosion potential move to the corrosion zones, where the AC damage occurred. Thus, according to Pourbaix diagram [17], it can be seen that a cathodically protected pipeline may be subjected to the four conditions, as shown in Figure 3.

Condition A (immunity domains): The potential of electrode potential is constant and lower than iron balance potential. It shows that the steel sample is under a good cathodic protection.

Condition B (iron may corrode but no hydrogen generation): The peak of fluctuant potential is between the iron balance potential and hydrogen balance potential domains.

Condition C (iron corrosion and hydrogen generation): The peak of fluctuant potential is between the hydrogen balance potential and oxygen balance potential domains.

Condition D (iron corrosion accompanied by oxygen generation): The peak of fluctuant potential exceeds the oxygen equilibrium potential.

Each test was performed in the DC current for 6 hours to make sure that the X70 specimens were under the cathodic protection before the AC experiments. The cathodic protection potential, was set at $E_C = -1.25 V_{SCE}$. Then, the corresponding AC potential was applied in the cathodic protection potential according to the Pourbaix diagram, insuring the AC/DC coupling peak potential was limited in the above mentioned four kinds of condition area. A regular observation of pH value was taken to

determine the pH variation in the surface soil under the synactic effect of the cathodic protection current and alternating current.

2.3 Electrochemical measurements

The electrochemical measurement used in the experiments was the classical three-electrode system. The reference electrode was Ag/AgCl electrode, while the auxiliary electrode was a titanium mesh electrode (the area was 30 cm²). The electrochemical test instrument is a PARSTAT 2273 electrochemical workstation incorporated with analyzing software Powersuit. The experimental device is placed in the GDJS-408 constant temperature humidity chamber. The working electrode was electro-reduced at -1.5 V for 3 minutes, while the temperature was kept at 25 °C.

The thermodynamic prediction of AC corrosion should be paid more attention in condition C and D, because the metal may suffer a serious corrosion problem. Therefore, the laboratory cyclic voltammetric tests were conducted to simulate low frequency AC corrosion in the two above mentioned conditions.

3. RESULTS AND DISCUSSION

3.1 Influence of AC on pH value of surface soil

Table 1 summarizes the changes of the soil pH value, and the Figure 4 shows the pH value of the X70 steel surface soil with the corrosion time.

Table 1. The pH value of X70 steel surface of the thin layer of soil simulated solution

Test conditions	Stabilization pH	Electrochemical measurements
Condition A Below $E_{Fe^{2+}/Fe}$	14.23	$E_C = -1.25 V_{SCE}$
Condition B Between $E_{Fe^{2+}/Fe}$ and E_{H^+/H_2}	14.21	$E_{ACpeak} = -0.75 V_{SCE}$
Condition C Between E_{H^+/H_2} and E_{O_2/H_2O}	13.04	$E_{ACpeak} = 0.2 V_{SCE}$
Condition D Above E_{O_2/H_2O}	11.15	$E_{ACpeak} = 1.2 V_{SCE}$

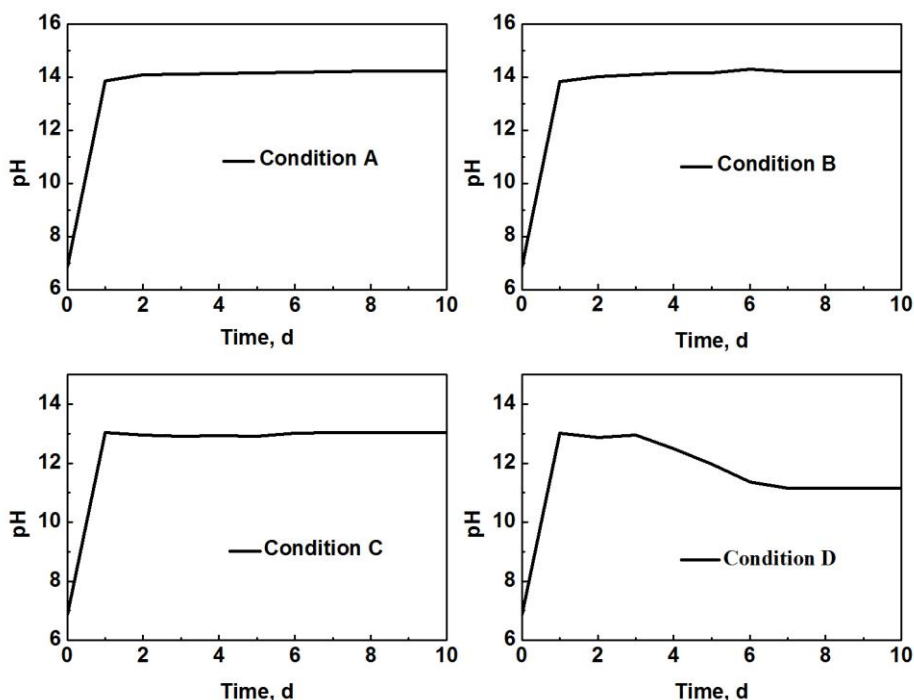
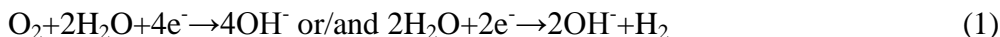


Figure 4. Relationship between the pH of soil above X70 steel surface

We will analyze the variation and the reasons of the pH value of the X70 steel surface soil under the above mentioned four conditions in turn.

Condition A: The pH value of the surface soil is relatively constant and remains at 14 in the whole corrosion process, as a result of the following reaction:



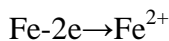
An increasing OH⁻ ion alkalinizes the surface soil and raises the pH value. When the pH value remains stable, the electrode potential is in ferrate domain. In this condition, we do not observe a corrosion phenomenon on the X70 steel surface. It indicates that the reaction kinetics of the ferrate generation are low, and the X70 steel is under a well cathodic protection.

Condition B: The whole process is similar with the Condition A, and the pH value also remains at 14. From the point of view of thermodynamics, a small amplitude of the potential oscillation appears on the X70 steel/soil interface. The electrode potential oscillates through the immunity domain - ferrate domain - passivation domain over and over. The corrosion almost never happens if the metal surface covered with a good protective oxide film. However, the corrosion may occur while the metal surface is not covered completely with a passive film. Because, even a small amplitude of the potential oscillations can reduce the oxide layer or destroy the formation of the passive film.

Condition C: The pH value is around 13 in the whole corrosion process. The reason of the decrease of the pH value is that a higher anode potential causes the oxidation of the hydrogen adhere to the specimen surface formed at the cathode cycle. In this condition, the electrode potential oscillates through the corrosion domain - ferrate domain - immunity domain periodically. The hydrogen evolution reaction will occur if the electrode potential is higher than the equilibrium potential of the

hydrogen. The X70/soil interface suffers a potential oscillation with a large amplitude, resulting in the AC corrosion.

Condition D: In this case, the pH value gradually reduces and eventually stabilizes at about 11, which is lower than the other cases. The following reaction may occur:



This process consumes a certain amount of HCl, leading to the soil acidification. The X70/soil interface is subjected to a larger amplitude of the potential oscillation. The electrode potential oscillates through the corrosion domain - ferrate domain - immunity domain periodically. The oxygen evolution reaction will occur if the electrode potential is higher than the equilibrium potential of the oxygen. So the frequent and large amplitude potential oscillations lead to the X70 steel in the corrosion and over protection, which cause a more serious corrosion.

3.2 AC corrosion mechanism of X70 steel at cathodic protection

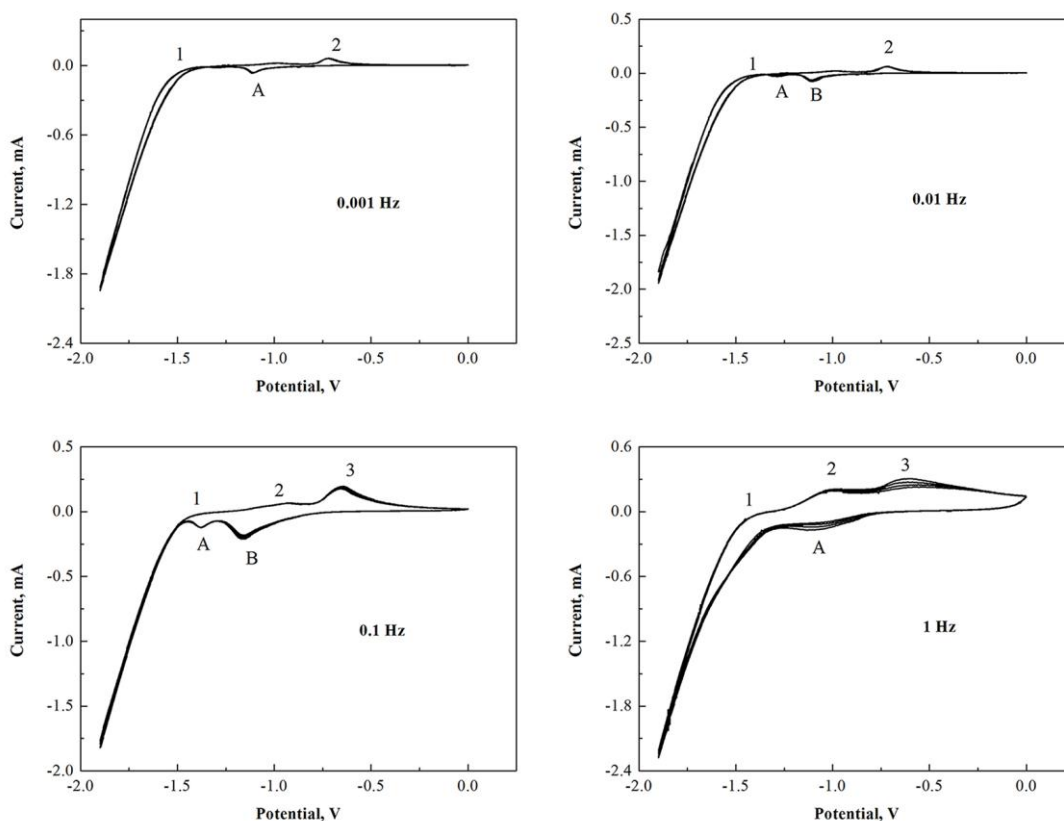


Figure 5. CV curves of X70 steel in soil solution at different sweep rate in condition C

The cyclic voltammetry technology is adopted to simulate the AC/DC coupling potential fluctuations. The initial potential was set to 0.95 V, by changing the highest and lowest scan potential to simulate the coupling potential of AC/DC in different domains. The scanning process was repeated

for 5 times, and by changing the scan rate to simulate the AC frequency. The detailed scan rate setting is as follows:

Condition C: 3.8 mV/s (0.001 Hz), 38 mV/s (0.01 Hz), 380 mV/s (0.1 Hz), 3800 mV/s (1 Hz), pH=13

Condition D: 7.8 mV/s (0.001 Hz), 78 mV/s (0.01 Hz), 780 mV/s (0.1 Hz), 7800 mV/s (1 Hz), pH=11

The volt-ampere characteristic curves of X70 steel are depicted in Figures 5-6 under the conditions C and D with different scanning rates.

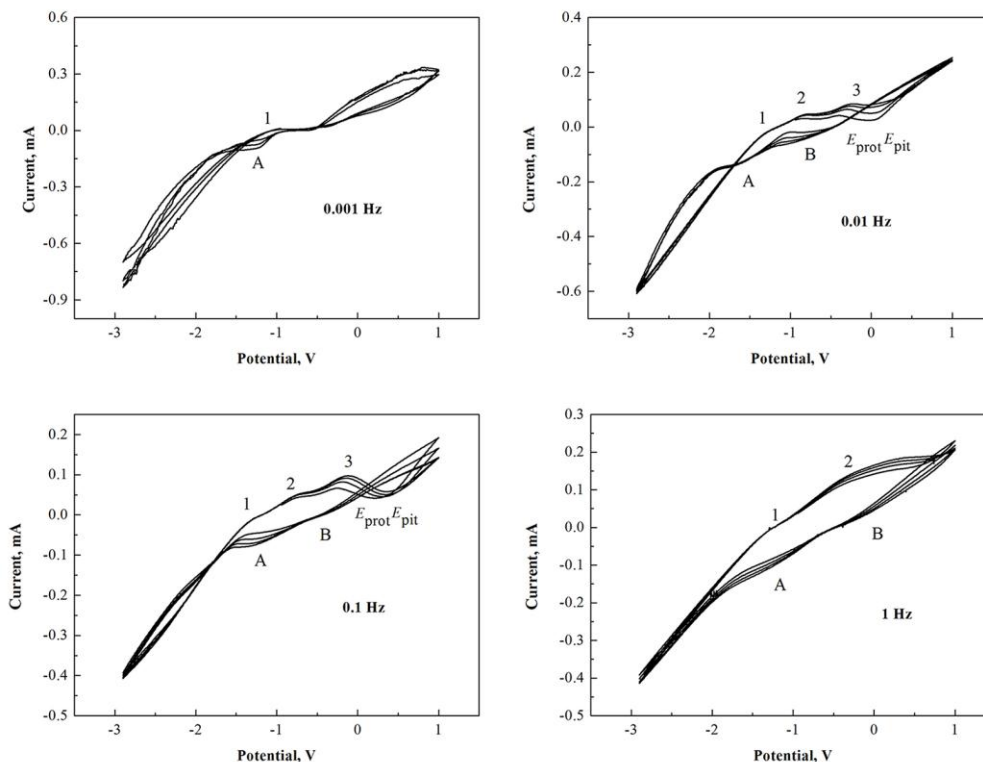


Figure 6. CV curves of X70 steel in soil solution at different sweep rate in condition D

If the superposition of the AC/DC voltage in the condition D drops to the Condition C, its volt-ampere characteristic curve will change, as shown in Figure 7.

To obtain the products components of X70 steel under AC corrosion, the XRD was employed to test the corrosive products after 10 days immersion experiment in an AC density of 100 A/m^2 . The X-ray diffraction was used by PANalytical X and the Theta was 0.001, minimum step size Omega was 0.001. The results were shown in Figure 8. The corrosive products mainly included the γ -FeO(OH), α -FeO(OH), α -Fe₂O₃, Fe₃O₄, FeCO₃.

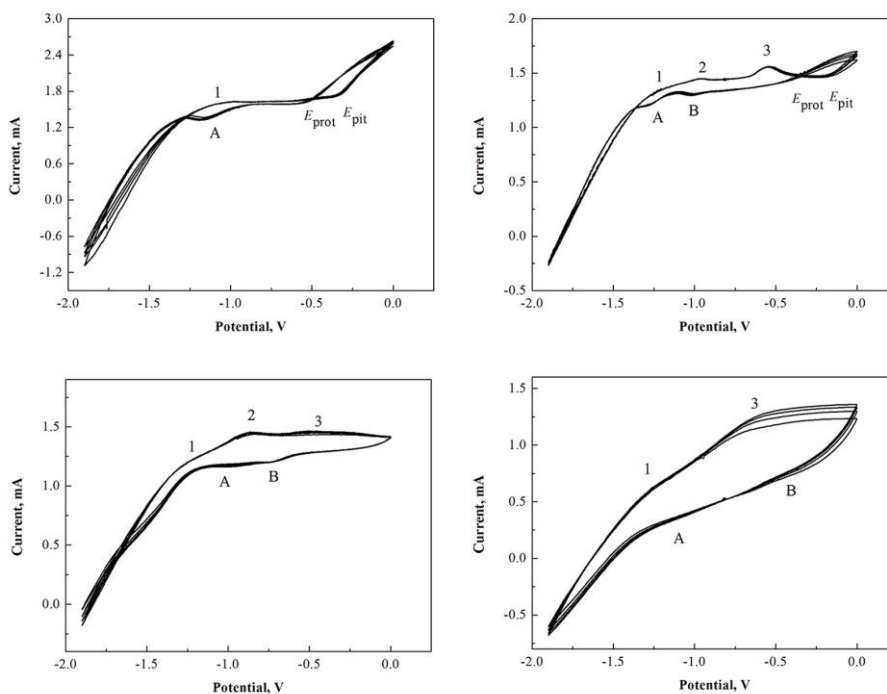


Figure 7. Cyclic voltammetry curves of X70 steel in soil solution at different sweep rate in condition D at pH=11

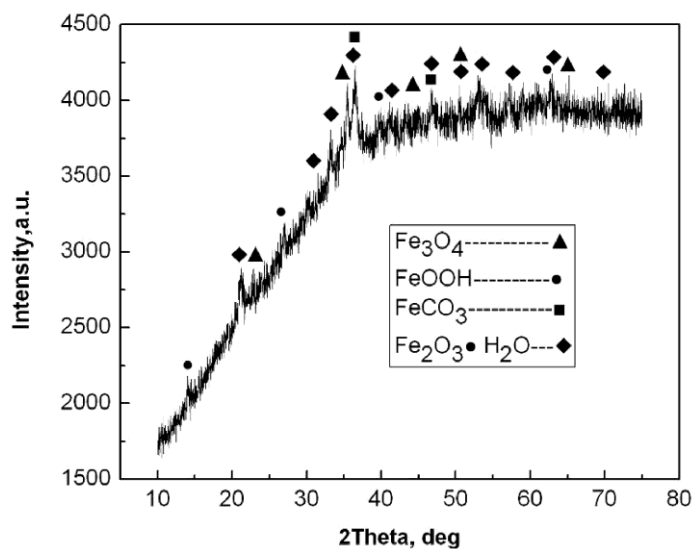


Figure 8. XRD patterns of corrosion products in simulated soil solution at 100 A/m² AC current density

In our corrosion experiments, the stratification state was observed in the AC corrosive product of X70 steel. The XRD tests demonstrated that the black rust layer directly stuck to the metal surface was the Fe₃O₄. The compounds of Fe²⁺, Fe³⁺ covered on the black rust layer, such as γ -Fe₂O₃, γ -FeO(OH) and so on. The outer layer was the red rust layer, and the main components included α -FeO(OH), α -Fe₂O₃ and FeCO₃ [18].

In condition C, the surface state of the specimen was observed to have a small change, including the appearance of some red corrosion products and decrease of the specimen weight. The phenomena can be explained by the volt-ampere characteristic.

In Figure 5, the current decreases continuously at first in a positive scanning. When the potential reaches the corrosion potential E_{corr} , the current changes and the first anodic peak 2 forms at the active dissolved area (products of $\text{Fe}(\text{OH})_2$ and FeCO_3 [19, 20]). The anodic current increases gradually after a slight decline with the increase of the anodic polarization potential, and correspondingly formed the anodic peak 3 (products of Fe_3O_4 and Fe_2O_3 [21]). Then, the corrosion process is about to enter the passivation stage, and the anode current maintains a stable value. When the anodic polarization potential exceeds the equilibrium potential of oxygen, the oxygen evolution reaction occurs. Along with the negative scanning of the potential, the cathodic peaks A and B form, which are the reduced products of the oxide at the anodic peaks 2 and 3.

Figure 6 describes the continuous decrease of the current at first in a positive scanning. When the potential reach the corrosion potential E_{corr} , the current changes and forms the first anodic peak 1 at the active dissolved area, producing $\text{Fe}(\text{OH})_2$ at this time. The current will increase suddenly, if the potential rises to the pitting corrosion potential E_{pit} . It shows that the pitting corrosion begins to form and grow gradually. When the potential regresses, the current gradually decreases to the critical passivation current and the potential will form a closed loop. The corresponding potential is the passivation potential E_{prot} , indicating that the formed pitting corrosion will be passivated again [22]. Along with the negative scanning of the potential, the corrosion product reduces and forms a cathodic peak A. The metal dissolution and hydroxide formation are determined by the diffusion in the potential range of anodic peak 2 (-1.2 V ~ 0.8 V). The voltage-current curves are quite different at various scanning rates. The increasing scanning rate shifts the E_{pit} forward. This is because the formation of the pitting corrosion requires a certain time, so that the Cl^- ion can damage the passive film and forms the core of the pitting corrosion on the metal surface.

Figure 7 shows that the voltage-current curves are quite similar, although the potential of the mixed AC and DC corrosion declines. It indicates that the metal still suffers the corrosion problem. Moreover, the corrosion of X70 steel slows when the AC frequency increases.

5. CONCLUSIONS

When the cathodic protection current existed without an AC interference, the metal surface soil was strong alkaline. In the pH range, the electrode potential stayed in the ferrate domain. The X70 steel was under a well cathodic protection because of the low reaction kinetics of the ferrate. The metal surface soil was also strong alkaline, although a small value AC was superimposed. The metal/soil interface suffered a small amplitude of the potential oscillation, reducing the oxide layer or destroying the formation of the passive film. If the metal/soil interface was subjected to a large amplitude of the potential oscillation, the pH value reduced, but the soil still presented a alkalinity. The electrode potential oscillated through the corrosion domain - ferrate domain - immunity domain periodically, leading to the AC corrosion.

Alternating current changed the original polarization potential and reduced the soil pH value. The periodic oscillation of potential destroyed the passive film, resulting in an asymmetric anodic oxidation and cathodic reduction curves. The superposition of the cyclical effect led to the anodic dissolution rate greater than the cathodic reduction rate, presenting a metal corrosion. Further, the electrode surface covered with a large amount of $\text{Fe}(\text{OH})_{\text{ads}}$, in the potential range of active dissolution of steel, resulting in the prior formation of hydroxides and oxides. During the different charge transfer, the hydroxide, as a corrosion inhibitor of the passive film, had an important impact on the metal corrosion.

ACKNOWLEDGEMENTS

This work was supported in part by the Natural Science Foundation of Jiangsu Province, China (No. BK20150270), the General Program of Natural Science Research Project of Jiangsu Province Universities and Colleges (No. 15KJB440001), and the Scientific Research Project of Changzhou (No. CJ20159034).

References

- 1 A. Soliz and L. Cáceres, *Int. J. Electrochem. Sci.*, 10 (2015) 5673.
- 2 K. M. Zohdy, *Int. J. Electrochem. Sci.*, 10 (2015) 414.
- 3 A. V. Sandu, A. Ciomaga, G. Nemtoi, M. M. A. B. Abdullah and I. Sandu, *Instrum Sci. Technol.*, 43 (2015) 454.
- 4 Y. Yang, Z. Li and C. Wen, *Acta Metall Sin.*, 49 (2013) 43.
- 5 E. Grigore, O. Pantea, D. Bombos, C. Calin, A. Bondarev and C. Gheorghe, *Rev. Chim.*, 66 (2015) 685.
- 6 C. Wen, J. Li, S. Wang and Y. Yang, *J. Nat. Gas Sci. Eng.*, 27 (2015) 1555.
- 7 M. A. Amin, S. Abdel Rehim, E. E. F. El-Sherbini and R. S. Bayoumi, *Int. J. Electrochem. Sci.*, 3 (2008) 199.
- 8 J. L. Wendt and D. T. Chin, *Corros. Sci.*, 25 (1985) 889.
- 9 D. Kuang and Y. F. Cheng, *Corros. Sci.*, 85 (2014) 304.
- 10 A. Popova, E. Sokolova, S. Raicheva and M. Christov, *Corros. Sci.*, 45 (2003) 33.
- 11 S. S. Abdel Rehim, O. A. Hazzazi, M. A. Amin and K. F. Khaled, *Corros. Sci.*, 50 (2008) 2258.
- 12 L.Y. Xu, X. Su, Z.X. Yin, Y.H. Tang and Y.F. Cheng, *Corros. Sci.*, 61 (2012) 215.
- 13 R. R. Fessler, A. J. Markworth and R. N. Parkins, *Corros.*, 39 (1983) 20.
- 14 J. Kim and Y. Kim, *Corros. Sci.*, 43 (2001) 2011.
- 15 L.Y. Xu, X. Su and Y.F. Cheng, *Corros. Sci.*, 66 (2013) 263.
- 16 R. Norsworthy, Proceedings of the 17th international corrosion congress, Las Vegas, Nevada, USA, October 6-10, 2008, paper No. 4017.
- 17 L.V. Nielsen, *CORROSION* 2005, Houston, Texas, USA, April 3-7, 2005, paper No. 05188.
- 18 Z. Panossian, S. Filho, N. de Almeida, M. Filho, D. Silva, E. Laurino, J. Oliver, G. Pimenta and J. Albertini, *CORROSION* 2009, Atlanta, Georgia, March 22-26, 2009, paper No. 09541.
- 19 J. Y. Zou and D. T. Chin, *Electrochim. Acta*, 33 (1988) 477.
- 20 J. Flis, H. Oranowska and Z. Szklarska-Smialowska, *Corros. Sci.*, 30 (1990) 1085.
- 21 M. Ergun and A. Y. Turan, *Corros. Sci.*, 32 (1991) 1137.
- 22 M. A. Deyab and S. T. Keera, *Egypt. J. Pet.*, 21 (2012) 31.